Marie Skłodowska-Curie (MSCA) – Innovative Training Networks (ITN)
H2020-MSCA-ITN European Training Networks

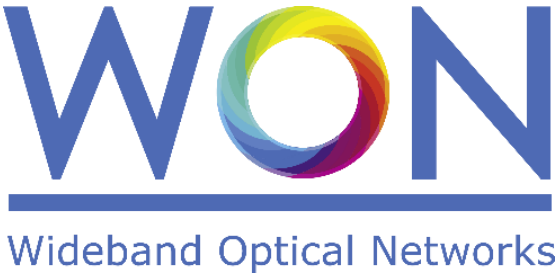

Wideband Optical Networks [WON]

Grant agreement ID: 814276

WP1 – Network management: planning and control

Deliverable D1.3 Techno-economic analysis of wideband optical transmission

This project has received funding from the European Union's Horizon 2020 research and innovation programme under the Marie Skłodowska-Curie grant agreement 814276.

Document Details

Work Package	WP1 – Network management: planning and control
Deliverable number	D1.3
Deliverable Title	Techno-economic analysis of wideband optical transmission
Lead Beneficiary:	Infinera Portugal (INF PT)
Deliverable due date:	30 June 2023
Actual delivery date:	27 June 2023
Dissemination level:	Public

Project Details

Project Acronym	WON
Project Title	Wideband Optical Networks
Call Identifier	H2020-MSCA-2018 Innovative Training Networks
Coordinated by	Aston University, UK
Start of the Project	1 January 2019
Project Duration	48 months
WON website:	https://won.astonphotonics.uk/
CORDIS Link	https://cordis.europa.eu/project/rcn/218205/en

WON Consortium and Acronyms

Consortium member	**Legal Entity Short Name**
Aston University	Aston
Danmarks Tekniske Universitet	DTU
VPIphotonics GmbH	VPI
Infinera Portugal	INF PT
Fraunhofer HHI	HHI
Politecnico di Torino	POLITO
Technische Universiteit Eidhoven	TUE
Universiteit Gent	UG
Keysight Technologies	Keysight
Finisar Germany GmnH	Finisar
Orange SA	Orange
Technische Universitaet Berlin	TUB
Instituto Superior Tecnico, University of Lisboa	IST

Abbreviations

AS:	Amplification site
ASE:	Amplified spontaneous emission
BP:	Best profile
EDFA:	Erbium-Doped Fibre Amplifiers
FF:	First fit
FWM:	Four-wave mixing
GA:	Genetic algorithm
GGN:	Generalized Gaussian Noise
GN:	Gaussian Noise
GSNR:	Generalized signal-to-noise ratio
LP:	Lightpath
MBT	Multi-band transmission
MF:	Multi-fibre
MCF:	Multi-core fibre
MMF:	Multi-mode fibre
NC:	No compensation
NF:	Noise-figure
NLI:	Nonlinear interference
OEO:	Optical-electrical-optical
OSNR:	Optical signal-to-noise ratio
PCE:	Path computation element
QoT:	Quality of transmission
RSA:	Routing and spectrum assignment
SNR:	Signal-to-noise ratio
SDM:	Spatial division multiplexing
SDN:	Software-defined networking
SNAP:	Statistical network assessment process
SRS:	Stimulated Raman scattering
SSFM:	Split-step Fourier method
SSMF:	Standard single-mode fibre
TDFA:	Thulium-Doped Fibre Amplifiers
UWB:	Ultra-wideband

CONTENTS

LIST OF FIGURES

EXECUTIVE SUMMARY

The present scientific deliverable “Techno-economic analysis of wideband optical transmission” is part of the Work Package 1 “Network management: planning and control” of the European Training Network “Wideband Optical Networks (WON)” funded under the Horizon 2020 Marie Skłodowska-Curie scheme Grant Agreement 814276.

This document provides details on the steps required to perform the optical performance evaluation of multi-band systems as well as the results of a techno-economic comparison between multi- and single-band systems.
The main topics addressed in this document are: (1) the efficient optical performance estimation and optimization, (2) network simulations and capacity-cost trade-offs analysis, and (3) techno-economic comparison of single- and multi-band systems.

1. Overview of multi-band optical line systems

The traffic transported in optical networks keeps increasing every year. Recent driving factors of the traffic expansion include the wider adoption of cloud computing and machine-to-machine communications, such as video surveillance, smart meters, and health monitoring [1,2]. This trend will be further reinforced by emerging technologies like 5G and 6G. Unfortunately, C-band only transmission systems are rapidly approaching the fundamental Shannon limit, which limits their capability to carry the offered traffic. The imminent capacity crunch can be resolved by exploring two promising approaches: increasing the transmission bandwidth of existing systems through multi-band transmission (MBT) and/or increasing the number of parallel spatial paths. This can be achieved by employing spatial division multiplexing (SDM) with multi-fibre (MF), multi-core/mode fibre (MMF/MCF), or few-mode fibre (FMF) transmission [3]. It is important to notice that MBT and SDM are not mutually exclusive. MBT is a technique that maximizes the per-fibre transmission, which can be combined with SDM by activating additional fibres when needed.

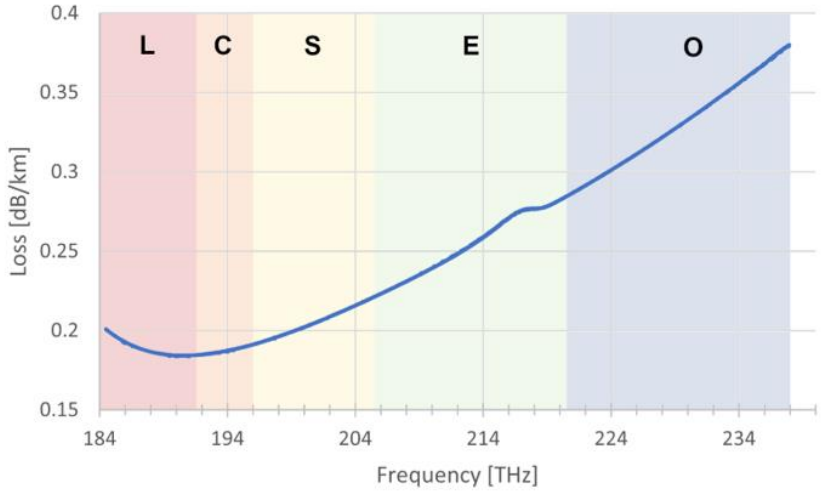

Figure 1: Attenuation coefficient for the ITU-T G.652D fibre from the L- to the O-band.

The widely deployed ITU-T G.652D fibre offers a low-loss transmission spectrum of ~54 THz from the O- to the L-band (see Figure 1), offering more than a ten-fold increase of the available bandwidth of C-band only systems (4.8 THz). An important question that must be answered is the identification of the spectrum bands of interest in MBT systems, i.e., which bands are economically viable. Because of the lower performance of bands beyond C and L, it is unlikely that the whole low-loss spectrum (from the L-band to the O-band) will be utilized [4]. Solutions for C+L-band transmission are already commercially available. However, deploying even wider transmission bandwidth systems is a matter of debate with ongoing research efforts aiming to develop devices operating in transmission bands beyond C+L. Transmission bands other than C and L require new amplification and switching technologies that are not yet mature enough for commercial utilization. The next band with highest potential to be exploited is the S-band (usually split in half, with S1-band and S2-band referring to the lower and higher frequencies of the S-band, respectively), which still shows similar optical fibre parameters as the C- and L-bands and can benefit from developments in ultra-wide-band amplification technologies such as thulium-doped fibre amplifiers (TDFA) [5].

In the meantime, analytical models that include the stimulated Raman scattering (SRS) effect have been used to predict multi-band transmission systems' performance and benefits [6-8]. An alternative and more accurate way to predict the performance of an optical transmission system is to use the

Split-step Fourier method (SSFM) to solve the nonlinear Schrodinger's propagation equation in the optical fibre. However, the computation time of SSFM may be prohibitive, especially when considering ultra-wideband (UWB) transmission systems [7].
These analytical models usually rely on the assumption that the nonlinear distortions behave as an additive Gaussian noise and estimate the quality of transmission (QoT) of a lightpath using the generalized signal-to-noise ratio (GSNR). The GSNR includes the effect of the additive Gaussian disturbances introduced by the optical amplifiers (amplified spontaneous emission - ASE) and the nonlinear interference (NLI) due to the self- and cross-channel nonlinear crosstalk resulting from optical fibre propagation. The GSNR is given by:

$$GSNR_i = \frac{P_i}{P_i^{ASE}+P_i^{NLI}},$$

where P_i is the received power of channel i and P_i^{ASE} and P_i^{NLI} are the power of the Gaussian noise corresponding to the ASE and the nonlinear interference at channel i, respectively. By combining the per-channel GSNR values and the required optical signal-to-noise ratio (OSNR) of transceivers, one can perform networks simulations to estimate the capacity and cost of MBT systems.
Achieving a cost-effective widespread Internet access requires a transformation of networks from closed and inflexible systems to open and adaptable ecosystems, as outlined by the software-defined networking (SDN) paradigm [9]. To progress towards programmable networks, it becomes essential to break down network architectures into independent elements that can be sourced from different vendors. Each disaggregated network element (NE) serves as a programmable white box, offering open models for its control and enabling virtualized access to its functionalities. These NEs are managed by a centralized multi-layer hierarchical network controller [10]. Within this context, it would be useful if we could optimize the GSNR on a span-by-span basis. This characteristic corresponds to assuming that nonlinearities accumulate incoherently along a given lightpath. This approximation has proven to be quite accurate in coherent-detection-based optical communication systems [10].

A proper QoT optimization is fundamental to estimate the cost of MBT system and make reliable comparisons against other capacity-enhancing solutions. Moreover, fast and accurate QoT estimation models are required to perform QoT optimization in a reasonable timeframe [11]. The initial sections of this deliverable are dedicated to detail the steps required to have a proper techno-economic analysis of MBT systems. Section 2 compares the accuracy and complexity of different QoT estimation algorithms. Section 3 describes the launch power optimization and other solutions to further increase the capacity of MBT systems. Section 4 presents the details of network simulations. A techno-economic analysis and comparison of single- and multi-band systems is presented in Section 5. Lastly, Section 6 describes the main conclusions of this report.

2. Efficient Quality of Transmission Estimation

The computation time and accuracy of the QoT estimation are crucial for network optimization algorithms due to the high number of parameters that must be optimized. For example, the average per band launch power and tilt were optimized for a C+L+S-band system in [12] using a genetic algorithm (GA)-based optimizer which required 3660 QoT evaluations to find the optimal setting for a single fibre span. Efficient planning and management of wideband optical networks may prove impractical if time-consuming QoT estimation algorithms are adopted. A fast but still accurate way to estimate optical performance consists in using the Gaussian-noise (GN) model proposed in [13], at least for C-band only systems. For multi-band transmission systems, we need to properly model the NLI interaction with the stimulated Raman scattering (SRS). This nonlinear effect plays a major role in such systems [14] and generates a power transfer from high to low frequency WDM channels during fibre propagation.

This work evaluates the computational time and accuracy of several alternatives for the estimation of the QoT of coherently detected signals in different transmission scenarios, namely considering C-, C+L-, S1+C+L- and S+C+L-band transmission. We compare different options for NLI and power evolution estimation leading to different trade-offs of accuracy and complexity. The considered nonlinear effect estimation methods are the numerical generalized Gaussian noise (GGN) model [6] and the analytical ISRS-GN [15], FWM [16] and enhanced FWM [17] models. The different strategies to estimate the power evolution of the channels are the simple exponential decay (ignoring the SRS effect), the analytical and numerical solutions of the SRS ODE system (SRS/Raman equations) and the sliding window technique [18]. The numerical GGN implementation available on GNPy library is used as reference.

The simulation setup is composed of a transmitter and a receiver connected by Ns spans of equal length (L). When more than one band is used for data transmission, a band demultiplexer is placed at the output of each fibre span to separate the transmitted bands and deliver them to the respective optical amplifiers, as shown in Figure 2a for an S+C+L-band system. After amplification, a band multiplexer combines the transmission bands.

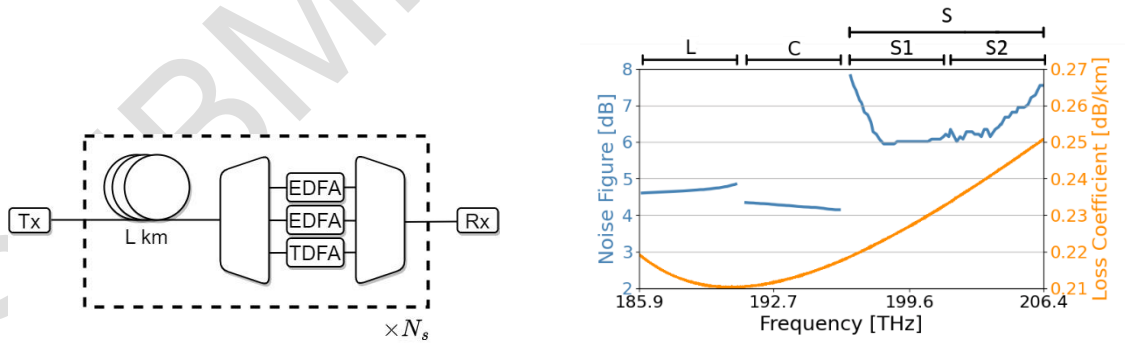

Figure 2: a) Simplified schematic of an Ns-span C+L+S MBT system. (b) Frequency-dependent fibre loss coefficient and amplifier's noise figure. The spectral occupation of each transmission band is also indicated.

Figure 2b shows the noise figures of the optical amplifiers and the spectral occupation of each transmission band. The data signals are modulated at 64 GBd, Nyquist-shaped with a roll-off factor of 0.15 and mapped into a 75-GHz spectrum grid with a 500-GHz guard band between adjacent bands. The transmission of a total of 64 channels is assumed in the C-, L-, S1 and S2-bands and 134 channels on the entire S-band. A Gaussian modulation format is assumed on all models, i.e., the modulation format correction term is set to zero on the ISRS-GN and FWM models. Fig. 2b also shows

the frequency-dependent loss coefficient of the optical standard single mode fibre (SSMF). Additionally, the fibre is characterized by a nonlinear coefficient of 1.27 W^{-1}/km and a dispersion parameter of 16.8 ps/nm/km at 1550 nm and a dispersion slope of 0.058 ps/nm^2/km. We consider input and output connector losses of 0.25 dB and insertion losses of the band DEMUX and MUX of 2 dB and 1 dB, respectively.

For the first set of results, shown in Figure 3, the GSNR after transmission along a 75-km span is calculated considering the different power evolution estimation methods and compared for three different transmission scenarios (C-, C+L- and C+L+S1-band transmission). A constant launch power per channel of −1 dBm is set in all cases. The GGN model is combined with the numerical solution of the Raman equations for the estimation of the optical signal power at the output of the fibre. This result provides a benchmark GSNR value to validate the different approaches. The GGN is used as reference because using the potentially more accurate SSFM-based simulations for such wideband systems is not viable within a practical time frame. Moreover, the GGN model has proven to be usually quite accurate when it was validated using SSFM-based simulations for a few wideband cases (up to S1+C+L MBT systems [19]). We also considered the use of the ISRS-GN model combined with the exponential decay (ISRS-GN Exp.), and with the analytical (ISRS-GN Ana.) and numerical (ISRS-GN Num.) solutions of the Raman equations to estimate the optical power at the output of the fibre.

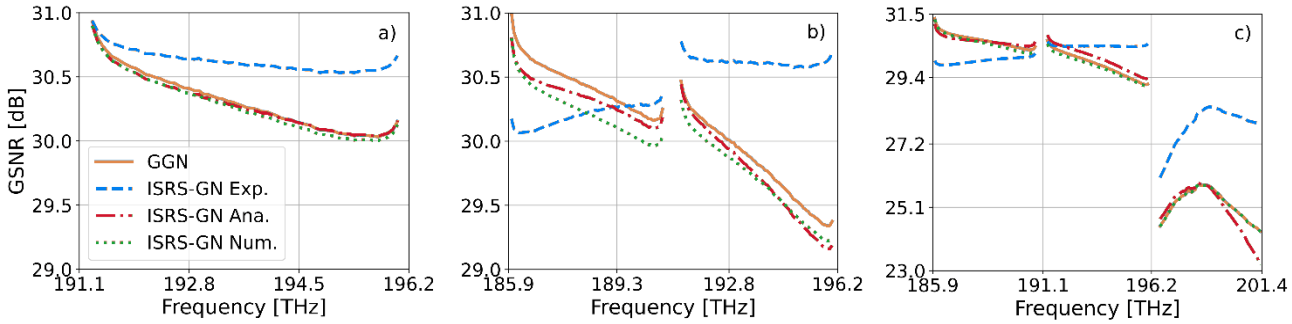

Figure 3: Estimated GSNR for (a) C-band (b) C+L-band (c) C+L+S1-band transmission at a constant launch power of -1 dBm.

These results show that, to achieve a good estimate of the GSNR, the power transfer between channels due to SRS must be considered. Even in the C-band-only transmission scenario, where the estimated NLI power is very similar independently of the method considered to calculate it, we find that using the exponential decay for the power evolution in the fibre may already lead to a GSNR estimation inaccuracy that may attain 0.5 dB. On the other hand, using the analytical or numerical solutions of the Raman equations combined with the ISRS-GN model led to a GSNR estimation error smaller than 0.05 dB. For the C+L-band transmission case, the GSNR estimation error exceeded 1 dB for a few channels when using the exponential decay model, whereas the analytical and numerical solutions of the Raman equations led to estimation errors not exceeding 0.25 dB for all channels. Moreover, Figure 3 shows that the GSNR profiles estimated by the ISRS-GN model combined with the analytical and numerical solutions of the Raman equations are very similar for the C-band only and C+L-band transmission scenarios. However, in the C+L+S1-band scenario, it can be noted that the analytical model underestimated the GSNR for the higher frequencies by more than 1 dB when compared to the one predicted by the GGN model. In this case, there is an overestimation of the power transfer due to SRS resulting from the linear approximation of the Raman gain for frequency separations exceeding 13 THz. This approximation error becomes particularly relevant for spectral separations wider than 15 THz.

The next set of results gives a more detailed evaluation of the accuracy of the models on wider bandwidth systems, i.e., the S1+C+L- and S+C+L-band systems (around 15 THz and 20 THz, respectively). We consider the ISRS-GN model combined with the numerical solution of the Raman equations and include the results for the FWM model combined with the sliding window technique and the eFWM model with the numerical solution of the Raman equation since these approaches potentially lead to a good trade-off between computation time and accuracy for these transmission scenarios. The GGN model combined with the numerical solution of the SRS ODE system is used as a reference. The results using the exponential decay and the analytical solutions of the Raman equations are not considered because they fail to correctly model the SRS effect in scenarios with more than 15 THz of transmission bandwidth.

The same ASE noise power as in the GGN model is calculated when using the ISRS-GN and the enhanced FWM models because the SRS power transfer is estimated using the same numerical solver. In these cases, only the NLI power estimate changes. However, for the FWM model, the estimation of the Raman effect also impacts the ASE noise power calculation.
The results depicted in Figure 4 and Figure 5 show the GSNR estimation error after transmission along 10 spans of fibre. The data was generated by independently varying the per channel launch power in the −2 to 4 dBm range in steps of 1 dB and the span length (L) between 50 and 100 km in steps of 10 km.

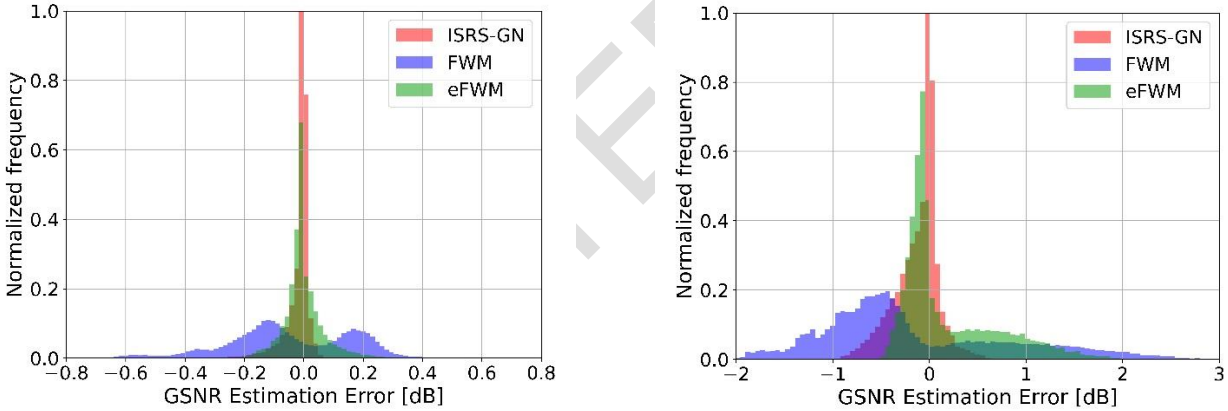

Figure 4: Normalized histogram of the error of GSNR estimation for the S1+C+L-band system for power per channel values between (a) -2 dBm and 1 dBm and (b) 2 dBm and 4 dBm.

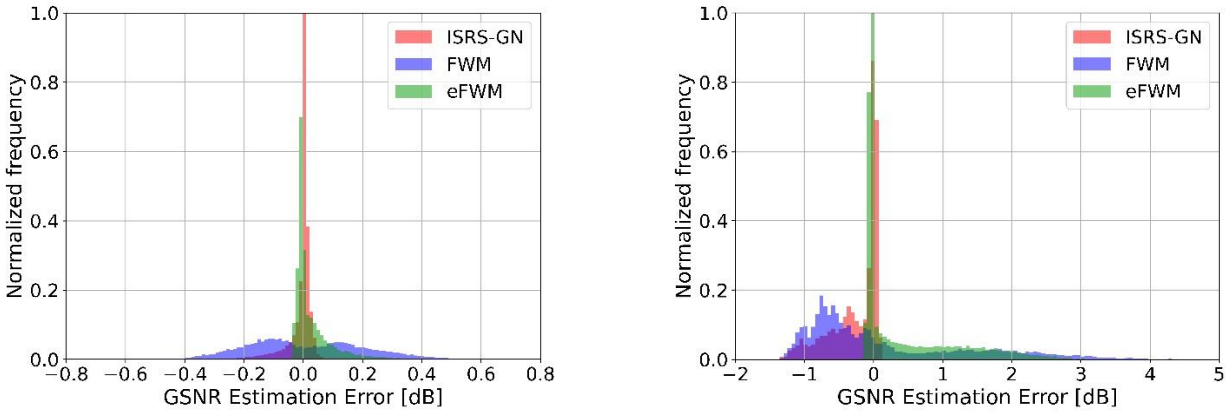

Figure 5: Normalized histogram of the error of GSNR estimation for the S+C+L-band system for power per channel values between (a) -2 dBm and 1 dBm and (b) 2 dBm and 4 dBm.

Figure 4a and Figure 5a show the normalized histogram of the error of GSNR estimation for both MBT scenarios for power per channel values ranging between −2 and 1 dBm, whereas Figure 4b and Figure 5b show the same histograms but for power per channel values ranging between 2 and 4 dBm. Looking at the results for the S1+C+L MBT system, we find that the closed-form ISRS-GN model provides the most accurate results even though similar accuracy is observed when using the eFWM model. For the lower launch power cases, the ISRS-GN model shows a maximum overestimation of the GSNR of only 0.1 dB and an underestimation of 0.4 dB. This result shows the importance of accurately estimating the NLI and the Raman gain even when the NLI power is low, i.e., the system is operating in a close-to-linear regime. For higher launch powers, the estimation inaccuracy ranges between −1.4 and 1 dB, whereas the standard FWM and the eFWM models show errors exceeding 2 dB. The maximum observed GSNR estimation errors were [1.4, 4.3, 3.1] dB for the ISRS-GN, FWM and eFWM models, respectively. Similar conclusions are drawn for the S+C+L MBT system, although with a slightly higher magnitude of errors. Interestingly, although the eFWM shows a higher number of cases with approximately 0 dB error than the other models for higher launch powers, its error variance is higher than when using the ISRS-GN model.

The closed-form ISRS-GN model combined with the numerical solution of the Raman equations displayed the best trade-off between computation time and accuracy in the evaluated scenarios. It is roughly 10000 times faster than the numerical GGN and has good accuracy for a bandwidth of up to 20 THz and moderate launch power levels. Some alternative methods are faster, such as the ISRS-GN model combined with the exponential decay or combined with the analytical solution of the SRS equations, but they exhibit worse accuracy on wideband systems and high launch powers. The eFWM model combined with the numerical solution of the Raman equations shows similar accuracy to the ISRS-GN, but it is roughly 100 times slower.

3. Optical Performance Optimization

The launch power optimization plays a key role in maximizing the GSNR and, consequently, the capacity of a transmission system, especially when using MBT. In this deliverable, the tilt and offset strategy is used to optimize the launch power. This is a practical engineering strategy that enables maximizing the QoT uniformity over the used spectrum [20]. Figure 6 presents an illustration on how this strategy is implemented in an S+C+L-band system. The optimization variables are parameters that can be typically set on commercial amplifiers: the per-band average channel power (P_x) and tilt (T_x). The power of a channel i of band x is given by $P_{\{i,x\}} = P_x + T_x(f_i - f_x)$, where f_i and f_x are the frequency of channel i and the centre frequency of band x, respectively. Positive tilts are represented in all bands in this figure.

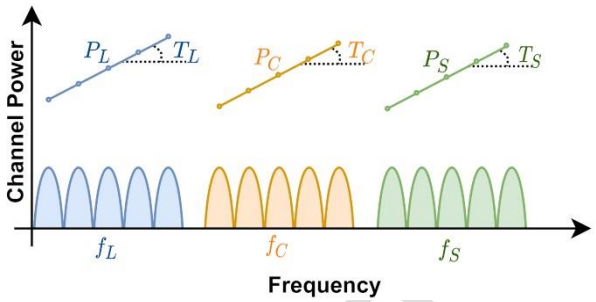

Figure 6: Illustration of the optimization variables.

The power optimization is performed to maximize the sum of the GSNR of all channels and minimize the GSNR ripple of each band considering full spectral load. This optimization problem in the presence of SRS is non-convex [8], and most publications have solved the optimization problem through explicit enumeration [21, 22], iterative [23, 24] or genetic algorithms [20, 25].

To illustrate the benefits of power control in multi-band systems, Figure 7 shows the GSNR profile after transmission in a 75-km span comparing the best profile (BP) with the GSNR profile obtained when using the LOGO power optimization approach per band, i.e., without any launch power tilt (no compensation-NC). The same C+L+S1 MBT scenario as in the previous section is considered in this case.

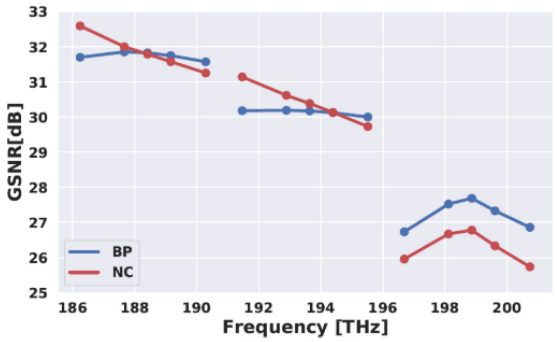

Figure 7: 75-km-span GSNR profiles comparing launch power control (Best profile – BP) with flat input power (no compensation – NC).

It can be noticed that, when using the launch power with power control, the GSNR ripple is almost completely removed from L- and C-band, while keeping approximately the same average GSNR. Regarding the S1-band, the launch power control strategy allows increasing the average GSNR by almost 1 dB while keeping similar GSNR ripple.

The performance of the S1-band may be highly impacted by the SRS, especially in highly loaded networks. This has a twofold impact: (I) the worse optical performance restricts the utilization of the

S1-band to shorter-reach lightpaths and/or lower-order modulation formats; and (II) the different optical performance within and between bands adds complexity to the routing and spectrum assignment (RSA) algorithms that run in the path computation element (PCE) used by the SDN controller. This limitation may be mitigated by optimizing the launch power profile in a way that all bands have similar GSNR [26]. For example, the launch power of the C- and L-band can be decreased to reduce the SRS power transfer and improve the GSNR of the S1-band. However, this approach reduces the system capacity and, therefore, should be avoided. Raman amplification can be used as an alternative solution to improve the performance of the S1-band [24].

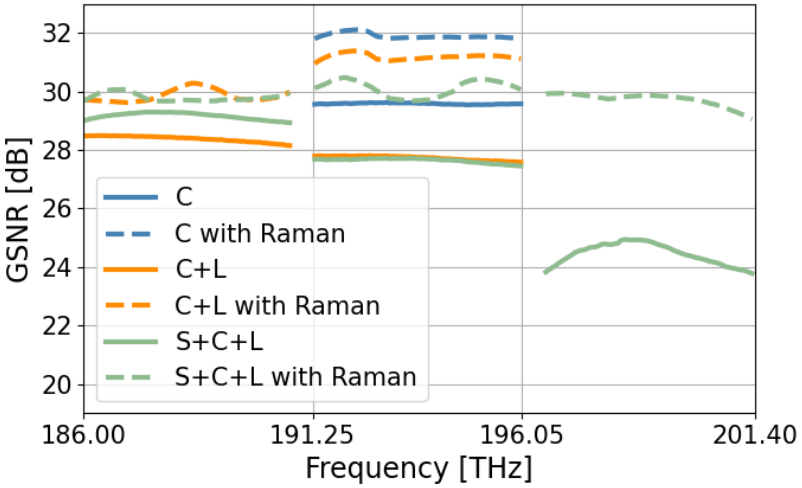

Figure 8: Optimized per-channel GSNR for an 80-km span.

Figure 8 shows the GSNR profiles of the analysed MBT systems after transmission in an 80-km span. To improve the optical performance of the S1-band, we deployed counter-propagating Raman amplification with an optimized frequency and optical power of the pump of 212 THz and 900 mW (measured at the optical fibre input), respectively. This strategy results in an improvement of the average GSNR in the S1-band from 24.5 dB to 29.7 dB. Moreover, the GSNR ripple is also reduced. These results show that adding a counter-propagating Raman pump to the transmission system is an effective way to compensate for the impact of SRS, the worse NF of the S-band amplifier, and the losses from the band DEMUX and MUX. Moreover, exploiting Raman amplification in combination with optimizing the launch powers with the proposed algorithm enables similar performance on all three bands, each comparable to that of the C-band only transmission system without Raman amplification. As expected, in the other scenarios (C+L- and C-band only), Raman amplification also enables to increase the GSNR, although the improvements are less dramatic than those observed in the S1+C+L-band system. The objective function of the optimization approach may be changed to impose a smaller variation of GSNR on all scenarios, but this strategy may lead to a reduction of the mean GSNR. Using additional Raman pumps can also be explored to flatten the received GSNR, but with higher optimization complexity. For wider transmission bands, i.e., a higher number of transmission bands, multiple Raman pumps must be used due to the extent of frequencies that need improvement.

Another solution to increasing the spectral efficiency of a transmission system consists in reducing the average span length of the network by splitting each span in half and adding a new amplification

site (AS) [27]. Figure 9 shows the optimized GSNR profiles after transmission on a single 80-km span or two 40-km spans, the latter being for the AS optimization scheme (C+L+S New AS).

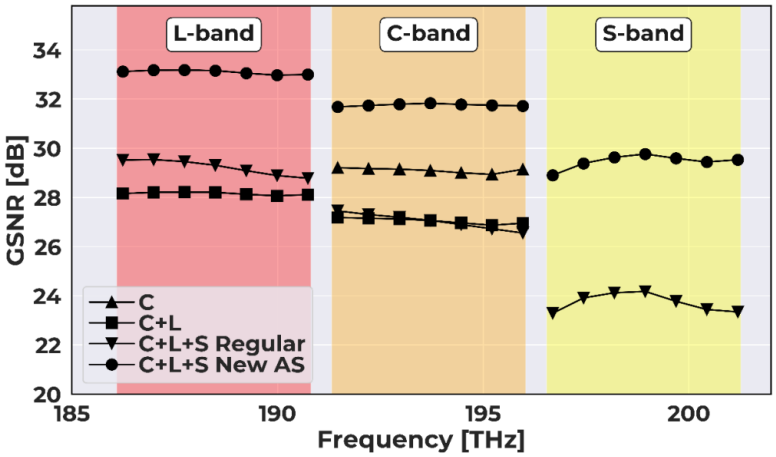

Figure 9: Optimized GSNR profiles for an 80-km span or two 40-km spans.

As expected, by splitting the span in half and transmitting along two spans, the performance of all transmission bands is improved, with the minimum GSNR of the [L, C, S1]-bands increasing by about [3.4, 2.9, 5.2] dB, respectively. This is a very relevant optical performance improvement but comes at the expense of requiring the deployment of a completely new optical amplification site, at the high cost of all the involved logistics. Moreover, this strategy does not equalize the GSNR of the different bands.

Another strategy to increase the spectral efficiency (that does not equalize the performance of the optical bands) is using a translucent instead of a transparent network design [28,29]. A translucent network design consists in enabling regeneration of the optical signal in intermediate nodes. In this case, we assume the use of 3R regenerators, where optical-electrical-optical (OEO) operation is performed. Different 3R regenerator placement algorithms may be used, e.g., aiming in maximizing the spectral efficiency of lightpaths (LP) but also considering the higher cost resulting from deploying the 3R regenerators.

4. Network Simulation

The next step towards a techno-economic evaluation is calculating the amount of traffic that a network supports given the per-channel GSNR for each transmission system. We use the statistical network assessment process (SNAP) [30] framework to retrieve the statistical dynamic metrics of the network, such as allocated capacity for a given blocking probability. Different strategies for routing and spectrum assignment may be used. The SNAP uses previously calculated per-span GSNR profiles to compute the GSNR of each lightpath, following a disaggregated approach. If the computed GSNR is higher than the required signal-to-noise ratio (SNR) plus an additional system margin, the lightpath is considered feasible. The transceiver modes of operation and corresponding required OSNR values are depicted in Table 1. The $OSNR_{req}$ is converted to required SNR as indicated in [31].

Mod. Format	QPSK	8QAM	16QAM
Bit rate [Gb/s]	200	300	400
$\boldsymbol{OSNR_{req}}$ [dB]	17.0	21.0	24.0
$\boldsymbol{SNR_{req}}$ [dB]	24.1	28.1	31.1

Table 1: Required OSNR for each transceiver operation mode.

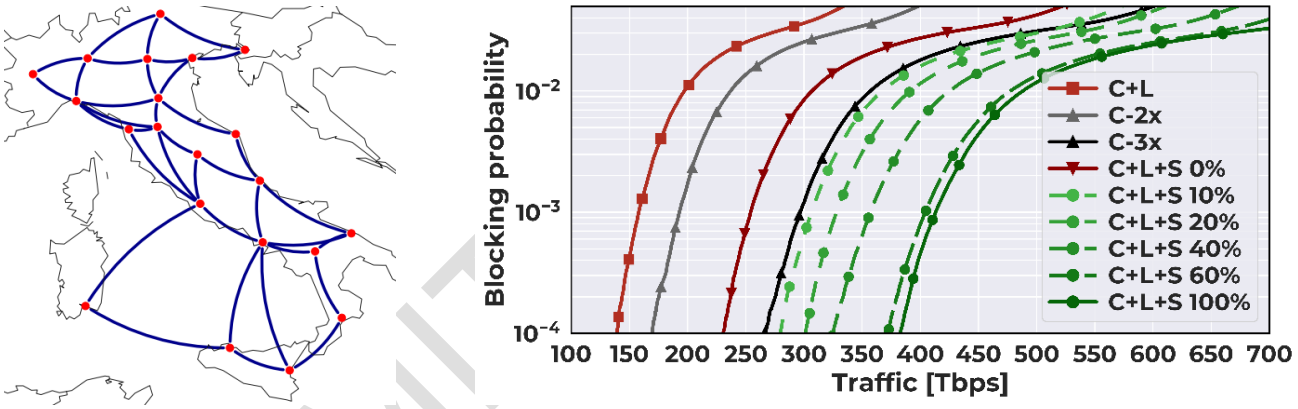

Figure 10: (a) Italian network topology and (b) Deployed traffic versus blocking probability.

As referred, the SNAP framework outputs the average blocking probability for a given deployed traffic load. To illustrate this process, we present results for C-, C+L- and C+L+S1-band systems in the Italian network topology (Figure 10a) with 21 nodes, 35 bidirectional links, an average link length of 209 km, and an average node degree of 3.4. We also consider the S1+C+L MBT system with the AS upgrade strategy. The per-span GSNR values are shown in Figure 9. The SNAP routing policy used is the k-shortest paths algorithm with k_{max}= 5, whereas the First-Fit (FF) approach is used as wavelength assignment policy. All established connections are fully transparent, and a system margin of 1 dB is considered. We assume that all spans of the network have 80 km and the new amplification site upgrade strategy splits the spans in half and adds a new amplifier for each transmission band. Deploying a new amplifier in only some specific transmission bands is not considered as most of the CAPEX will result from the extra amplification site infrastructure, and not necessarily from the optical amplifiers. The upgrade strategy progressively adds new amplification sites on the network and the priority of the links to be updated is determined based on the routing space of the network.

Figure 10b shows the blocking probability versus the network total allocated traffic. It considers the reference C+L scenario, C+L+S1 (0%), and the cases where 20, 40, 60% and 100% of the network spans receive an additional amplification site. It also presents capacity curves for C-band-only systems with 2 or 3 parallel fibres (C-2x and C-3x, respectively). At a blocking probability of 10^{-2}, the C+L MBT configuration supports 196.8 Tbps whereas the the C+L+S1 (0%) MBT system supports 306.5 Tbps. Therefore, exploiting the S1-band leads to extending the network throughput by 56% compared to the reference C+L scenario. Moreover, C-2x supports 236.8 Tbps (20% increase) whereas the C-3x system supports 356.5 Tbps (81% increase). In the C+L+S1 100% case, the network capacity increases to 487.9 Tbps, which is 148% higher than the C+L MBT scenario. This huge capacity extension results from the higher QoT of this MBT scenario, consequently supporting more spectrally efficient modulation formats. Additionally, adding a new AS in only 10% of the spans slightly outperforms the multi-fibre system with the same number of channels (C-3x). However, all these solutions have different complexities and costs.

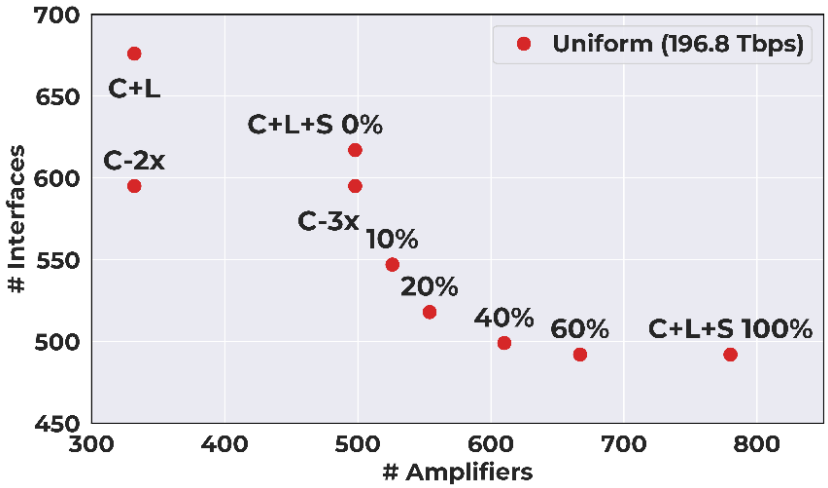

Figure 11: Total number of amplifiers versus the number of interfaces for the Italian network considering the strategy to build additional amplifications sites.

Figure 11 shows the number of required interfaces and the total number of amplifiers used for the deployed traffic corresponding to BP = 10^{-2} for the C+L scenario (196.8 Tb/s). The reduction in spectral efficiency resulting from enabling additional transmission bands is quite clear in this case. The reference C+L scenario requires the use of 676 optical interfaces whereas the C-band-only system with 2 parallel fibres (C-2x) requires 595. A total of 332 optical amplifiers are used in both cases (166 for each band/fibre). The C+L+S 0% scenario requires 617 interfaces whereas the C-3x requires 595 interfaces with both solutions requiring a total of 498 amplifiers. Interestingly, the C-3x used the same number of interfaces as the C-2x but required the same number of amplifiers as the C+L+S 0% scenario. The reduction in the number of interfaces from the C+L to the C+L+S 0% system is a consequence of the slightly higher GSNR levels in the L band and the specific traffic load which, since it does not correspond to a high traffic load, does not use channels in S-band because of the spectral allocation policy. In summary, the numbers of required interfaces were 547, 518, 499, 492, and 492 for C+L+S 10%, 20%, 40%, 60%, and 100%, respectively.

5. Techno-economic Analysis

The results of the previous section suggest that, because of the lower performance of bands beyond C and L, it is unlikely that the whole low-loss spectrum (e.g., from the L-band to the O-band) will be utilized in commercial systems. Instead, it is more realistic to assume that mid-term deployments will comprise C, L and one or a few other transmission bands that have reasonable performance. More details on the cost analysis of using those bands will be given in this section, highlighting in which conditions the deployment of additional transmission bands is cost-effective.

We consider the equipment cost shown in Table 2. The costs are given in arbitrary monetary units (m.u.) and, for simplicity, one m.u. corresponds to the cost of a C-band erbium-doped fibre amplifier (EDFA). We assume that the L-band amplifier has the same cost as the C-band counterpart. For the S-band amplifier, we consider a variable cost (C_S) between 1 and 2 monetary units. The cost of band multiplexers and demultiplexers is 0.04. Lastly, the fibre cost C_f (given in m.u. per kilometre) is assumed as variable to evaluate a higher range of transmission scenarios. C_f represents the cost of all expenses related to fibre deployment (materials, labour, equipment, etc.).

Equipment	Cost [m.u.]
C-band EDFA	1
L-band EDFA	1
S-band TDFA	C_S
Band MUX	0.04
Band DEMUX	0.04
Optical Fibre (per km)	C_f

Table 2: Equipment cost.

We analyse the cost evolution with increasing deployed traffic in the German network (DT topology), which consists of 17 optical nodes and 26 links with an average length of 246 km (
Figure 12a). We consider single- and multi-band systems with transmission bandwidths from 4.8 THz to 20 THz (i.e., S2+S1+C+L-band) since day 1 and the deployment of additional parallel fibres in the most congested links to cope with the increasing traffic. The best combination of transmission bands was selected for each system (with one, two, three and four transmission bands in total) to maximize the system capacity. The SNAP routing policy comprises the k-shortest paths algorithm with k_{max}= 1 and the First-Fit (FF) approach for wavelength assignment. All established connections are fully transparent, and a 3-dB system margin is set. We consider that all spans of the network are 80 km long.

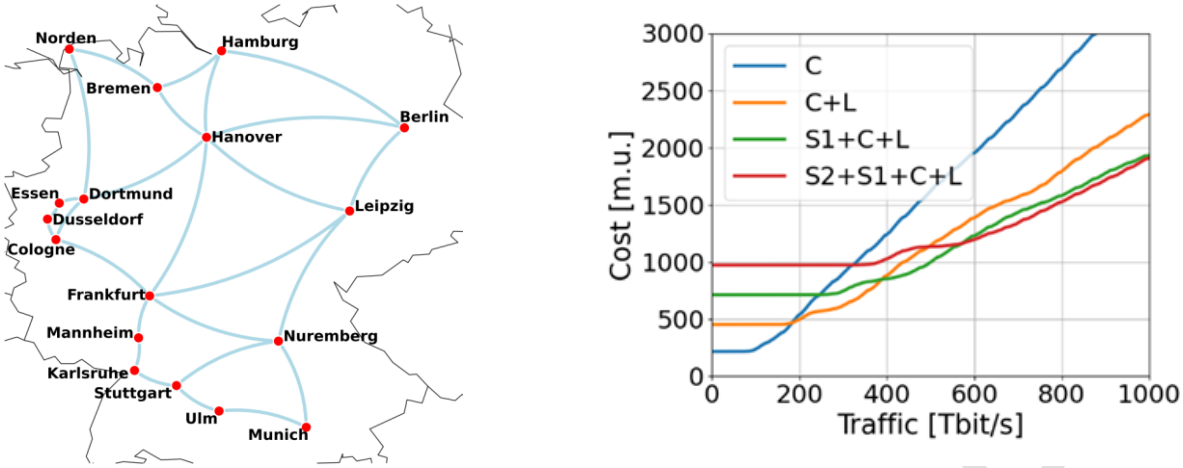

Figure 12: (a) DT network topology. (b) Amplifiers and fibre deployment cost evolution.

First, we assume that the S-band amplifiers cost 20% more than the C- and L-band amplifiers (C_S = 1.2 m.u.) and fibre deployment cost is 0.07 m.u./km, which is approximately the per-fibre cost of purchase and deployment of a Sterlite's 8-FC cable [32].

Figure 12b shows the evolution of the amplifiers and fibre deployment cost versus the traffic deployed on the network. The most cost-effective system depends on the traffic deployed on the network and the fibre deployment cost. The initial cost of the multi-band systems is higher mainly because of the higher number of amplifiers deployed since day one. To avoid the initial higher expenses of the multi-band systems, amplifiers may be deployed in a pay-as-you-grow approach, but this analysis remains for a future work. For higher deployed traffic loads, the C-band-only systems becomes more expensive than the other multi-band solutions because of the cost of the additional optical fibres required.

Figure 12b also shows the average deployed traffic when the first fibre upgrade is performed. For the C-band-only system, the first fibre upgrade is required at an average deployed traffic of 95 Tbit/s. For the multi-band systems, the initial higher cost is compensated by allowing a higher traffic load before requiring an optical fibre upgrade. Indeed, the supported traffic using just a single fibre per span is increased by 1.8, 2.9, and 3.3 times (to 175 Tbit/s, 274 Tbit/s and 314 Tbit/s) for C+L, S1+C+L, and S2+S1+C+L MBT systems, respectively. Note that, even though the S2+S1+C+L MBT system enables four times higher transmission bandwidth than the C-band-only system, the offered network capacity without using parallel fibres only increases by 3.3 times.

To have a better view of the trade-offs between fibre deployment, S-band amplifier cost and number of transmission bands,

Figure 13a and

Figure 13b highlights the cheapest transmission system for each combination of C_S and C_f for a deployed traffic of 600 Tbit/s and 1000 Tbit/s, respectively. Assuming that the network capacity in day one is 95 Tbit/s (traffic deployed on the C-band-only network when the first fibre upgrade is required) and that traffic grows by 30% every year, a deployed traffic of 600 Tbit/s is reached in less than 5 years and 1000 Tbit/s in less than 9 years.

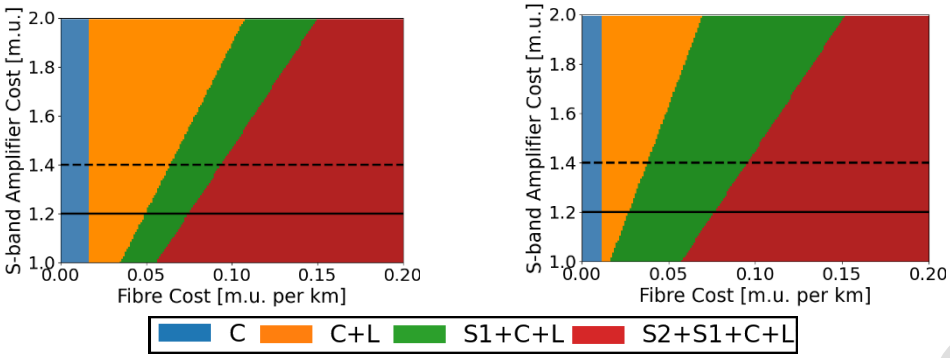

Figure 13: Cheapest transmission system for different combinations of fibre deployment and S-band amplifier costs for a deployed traffic of (a) 600 Tb/s and (b) 1000 Tb/s.

The analysis of Fig.13 shows that using the C-band-only system is preferable when the fibre deployment cost is low, independent of the cost of the S-band amplifiers. This case corresponds, e.g., to the scenario where dark fibre has been deployed and is still available. This result is a consequence of the worse optical performance resulting from enabling additional transmission bands. In summary, a multi-fibre system will typically be the most interesting upgrade solution when it can be deployed at the same optical network infrastructure cost since it enables higher capacity/spectral efficiency than the corresponding MB approach. Using additional transmission bands becomes more attractive when the cost of the fibre deployment increases. As an example, for a fixed S-band amplifier cost of 1.2 monetary units and a deployed traffic of 600 Tbit/s (solid line in
Figure 13a), the C-band system is the most cost-effective solution for a fibre deployment cost of up to 0.016 m.u./km, the C+L-band system is the most cost-effective solution for 0.016 m.u./km < C_f ≤ 0.050 m.u./km, then the S1+C+L system is the best solution for 0.050 m.u./km < C_f ≤ 0.074 m.u./km and, lastly, the four-band system is the best choice for fibre deployment costs higher than 0.074 m.u./km. For a higher cost of the S-band amplifiers such as 1.4 monetary units (dashed line in
Figure 13a), the region of interest of the C-band-only system remains unchanged but, as a consequence, the C+L-band system becomes the most attractive solution for a larger interval of fibre deployment costs (the C+L-band system is the cheapest for 0.016 m.u./km < C_f ≤ 0.064 m.u./km). The interval of interest of the three-band system is shifted to the right (the S1+C+L-band system is the cheapest for 0.064 m.u./km < C_f ≤ 0.093 m.u./km). When considering the 1000 Tbit/s deployed traffic, the multi-band systems become more attractive than for the lower traffic loads. For example, considering the S-band amplifier cost of 1.2 monetary units (solid line in
Figure 13b), the C-band-only interest region is reduced to fibre deployment costs of up to 0.011 m.u./km. The C+L-band system is the cheapest for 0.011 m.u./km < C_f ≤ 0.027 m.u./km, the S1+C+L system is the cheapest for 0.027 m.u./km < C_f ≤ 0.076 m.u./km and the four-band system is the best choice for fibre deployment costs higher than 0.076 m.u./km.

6. Conclusions

In this work, we presented several aspects required to perform fair and complete techno-economic comparisons between multi-band and multi-fibre-upgraded networks. A comparison of different models for optical performance evaluation was presented in section 2, highlighting that a fast and sufficiently accurate model is required for proper optimization and estimation of the optical performance of multi-band systems. Afterwards, section 3 presented the benefits of launch power optimization and strategies to increase the spectral efficiency of multi-band systems, which are fundamental to fully enable the potential of wideband transmission. Section 4 shows the trade-offs involved when upgrading an optical network in terms of number of amplifiers, interfaces, and network capacity. Finally, section 5 presents a techno-economic comparison of C-band-only systems and various multi-band systems, ranging from enabling between two and four 4.8-THz transmission bands. Results show that the best solution is highly dependent on the fibre deployment cost and the traffic load. Indeed, enabling additional transmission bands is more cost-efficient with the increasing of the fibre deployment costs and traffic load.

5. REFERENCES

[1] Cisco, “Cisco annual internet report (2018–2023) white paper,” Tech report, Cisco (2020).

[2] M. Z. Chowdhury, M. Shahjalal, S. Ahmed, and Y. M. Jang, “6G wireless communication systems: Applications, requirements, technologies, challenges, and research directions,” IEEE Open J. Commun. Soc. 1, 957–975 (2020).

[3] P. J. Winzer, D. T. Neilson, and A. R. Chraplyvy, “Fiber-optic transmission and networking: the previous 20 and the next 20 years [invited],” Opt. Express 26, 24190–24239 (2018).

[4] A. Ferrari, A. Napoli, J. K. Fischer, N. Costa, J. Pedro, N. Sambo, E. Pincemin, B. Sommerkohrn-Krombholz, and V. Curri, “Upgrade capacity scenarios enabled by multi-band optical systems,” in 2019 21st International Conference on Transparent Optical Networks (ICTON), (2019), pp. 1–4.

[5] A. Souza, N. Costa, J. Pedro and J. Pires, "Raman Amplification for Simplified Channel Provisioning in Wide-Band Optical Networks," 2022 Optical Fiber Communications Conference and Exhibition (OFC), (2022), pp. 1-3

[6] M. Cantono, D. Pilori, A. Ferrari, C. Catanese, J. Thouras, J. Augé, and V. Curri, “On the interplay of nonlinear interference generation with stimulated Raman scattering for QoT estimation,” J. Light. Technol. 36, 3131–3141 (2018)

[7] D. Semrau, R. I. Killey, and P. Bayvel, “The Gaussian noise model in the presence of inter-channel stimulated Raman scattering,” J. Light. Technol. 36, 3046–3055 (2018).

[8] I. Roberts, J. M. Kahn, J. Harley, and D. W. Boertjes, “Channel power optimization of WDM systems following Gaussian noise nonlinearity model in presence of stimulated Raman scattering,” J. Light. Technol. 35, 5237–5249 (2017).

[9] W. Xia, Y. Wen, C. H. Foh, D. Niyato, and H. Xie, “A survey on software-defined networking,” IEEE Commun. Surv. Tutorials 17, 27–51 (2015).

[10] V. Curri, "GNPy model of the physical layer for open and disaggregated optical networking [Invited]," in Journal of Optical Communications and Networking, vol. 14, no. 6, pp. C92-C104, June 2022.

[11] A. Souza, B. Correia, N. Costa, J. Pedro and J. Pires, "Accurate and Scalable Quality of Transmission Estimation for Wideband Optical Systems," 2021 IEEE 26th International Workshop on Computer Aided Modeling and Design of Communication Links and Networks (CAMAD), Porto, Portugal, 2021, pp. 1-6, doi: 10.1109/CAMAD52502.2021.9617794.

[12] B. Correia, R. Sadeghi, E. Virgillito, A. Napoli, N. Costa, J. Pedro, and V. Curri, “Optical power control strategies for optimized C+L+S-bands network performance,” in 2021 Optical Fiber Communication Conference (OFC), (2021), pp. 1–3.

[13] P. Poggiolini, G. Bosco, A. Carena, V. Curri, Y. Jiang, and F. Forghieri, “The GN-model of fiber non-linear propagation and its applications,” J. Light. Technol. 32, 694–721 (2014).

[14] F. Hamaoka, M. Nakamura, S. Okamoto, K. Minoguchi, T. Sasai, A. Matsushita, E. Yamazaki, and Y. Kisaka, “Ultra-Wideband WDM Transmission in S -, C -, and L -Bands Using Signal Power Optimization Scheme,” J. Light. Technol. 37, 1764–1771 (2019).

[15] D. Semrau, R. I. Killey, and P. Bayvel, “A closed-form approximation of the Gaussian noise model in the presence of inter-channel stimulated Raman scattering,” J. Light. Technol. 37, 1924–1936 (2019).

[16] D. Uzunidis, C. Matrakidis, and A. Stavdas, “Closed-form FWM expressions accounting for the impact of modulation format,” Opt. Commun. 440, 132–138 (2019).

[17] A. Souza, N. Costa, J. Pedro and J. Pires, " Comparison of Fast Quality of Transmission Estimation Methods for C+L+S Optical Systems," in Journal of Optical Communications and Networking, *to be published*.

[18] D. Uzunidis, C. Matrakidis, E. Kosmatos, A. Stavdas, A. Lord, “On the benefits of power optimization in the S, C and L-band optical transmission systems,” Computer Networks, 211 (2022).

[19] A. D'Amico, B. Correia, E. London, E. Virgillito, G. Borraccini, A. Napoli, and V. Curri, "Scalable and disaggregated GGN approximation applied to a C+L+S optical network," J. Light. Technol. 40, 3499–3511 (2022).

[20] B. Correia et al., "Multiband Power Control Impact on the Transmission Capacity of Optical Line Systems," 2021 IEEE Photonics Society Summer Topicals Meeting Series (SUM), Cabo San Lucas, Mexico, 2021, pp. 1-2, doi: 10.1109/SUM48717.2021.9505860.

[21] E. Virgillito, E. London, A. D'Amico, B. Correia, A. Napoli, and V. Curri, "Single- vs. multi-band optimized power control in C+L WDM 400G line systems," in 2021 Optical Fiber Communications Conference and Exhibition (OFC), (2021), pp. 1–3.

[22] R. Sadeghi, B. Correia, E. Virgillito, A. Napoli, N. Costa, J. Pedro, and V. Curri, "Performance comparison of translucent C-band and transparent C+L-band network," in Optical Fiber Communication Conference (OFC) 2021, (Optical Society of America, 2021), p. M3E.4.

[23] F. Hamaoka, M. Nakamura, S. Okamoto, K. Minoguchi, T. Sasai, A. Matsushita, E. Yamazaki, and Y. Kisaka, "Ultra-wideband WDM transmission in S-, C-, and L-bands using signal power optimization scheme," J. Light. Technol. 37, 1764–1771 (2019).

[24] A. Souza, N. Costa, J. Pedro and J. Pires, "Benefits of counterpropagating Raman amplification for multiband optical networks," in Journal of Optical Communications and Networking, vol. 14, no. 7, pp. 562-571 (2022).

[25] H. Buglia, E. Sillekens, A. Vasylchenkova, W. Yi, R. Killey, P. Bayvel, and L. Galdino, "Challenges in extending optical fibre transmission bandwidth beyond C+L band and how to get there," in 2021 International Conference on Optical Network Design and Modeling (ONDM), (IEEE, 2021), pp. 1–4.

[26] D. Uzunidis, C. Matrakidis, A. Stavdas and A. Lord, "Power Optimization Strategy for Multi-Band Optical Systems," 2020 European Conference on Optical Communications (ECOC), Brussels, Belgium, 2020, pp. 1-4, doi: 10.1109/ECOC48923.2020.9333398.

[27] B. Correia et al., " Optimized Amplification Sites Placement in Multi-band C+L+S Optical Networks," in 2023 International Conference on Optical Network Design and Modeling (ONDM), (IEEE, 2023), pp. 1–4.

[28] R. Sadeghi et al., "Performance Comparison of Translucent C-band and Transparent C+L-band Network," 2021 Optical Fiber Communications Conference and Exhibition (OFC), San Francisco, CA, USA, 2021, pp. 1-3.

[29] R. Sadeghi et al., "Transparent vs Translucent Multi-Band Optical Networking: Capacity and Energy Analyses," in Journal of Lightwave Technology, vol. 40, no. 11, pp. 3486-3498, 1 June1, 2022, doi: 10.1109/JLT.2022.3167908.

[30] V. Curri, M. Cantono, and R. Gaudino, "Elastic All-Optical Networks: A New Paradigm Enabled by the Physical Layer. How to Optimize Network Performances?" J. Light. Technol. 35, 1211–1221 (2017).

[31] R.-J. Essiambre and R. W. Tkach, "Capacity trends and limits of optical communication networks," Proc. IEEE 100, 1035–1055 (2012).

[32] Rana Kumar Jana, Anand Srivastava, Andrew Lord, and Abhijit Mitra, "Optical cable deployment versus fiber leasing: an operator's perspective on CapEx savings for capacity upgrade in an elastic optical core network," J. Opt. Commun. Netw. 15, C179-C191 (2023)